Available online at www.sciencedirect.com
SCIENCE DIRECT®
Polymer 44 (2003) 5023–5030
polymer
www.elsevier.com/locate/polymer

Dielectric spectroscopy on melt processed polycarbonate—multiwalled carbon nanotube composites

Petra Pötschke[a], Sergej M. Dudkin[b], Ingo Alig[b,*]

[a]*Institut für Polymerforschung Dresden e.V., Hohe Str. 6, D-01069 Dresden, Germany*
[b]*Deutsches Kunststoff-Institut, Schlossgartenstrasse 6, D-64289 Darmstadt, Germany*

Received 29 April 2003; accepted 3 June 2003

Abstract

Complex permittivity and related AC conductivity measurements in the frequency range between 10^{-4} and 10^{7} Hz are presented for composites of polycarbonate (PC) filled with different amounts of multiwalled carbon nanotubes (MWNT) varying in the range between 0.5 and 5 wt%. The composites were obtained by diluting a PC based masterbatch containing 15 wt% MWNT by melt mixing using a Micro Compounder. From DC conductivity measurements it was found that for samples processed at a mixing screw speed of 150 rpm for 5 min, the percolation occurs at a threshold concentration (p_c) between 1.0 and 1.5 wt% MWNT. For concentrations of MWNT near the percolation threshold, the processing conditions (screw speed and mixing time) were varied. The differences in the dispersion of the MWNT in the PC matrix could be detected in the complex permittivity and AC conductivity spectra, and have been explained by changes in p_c. The AC conductivity and permittivity spectra are discussed in terms of charge carrier diffusion on percolation clusters and resistor–capacitor composites.

Keywords: Multiwalled carbon nanotube composites; Percolation; Dielectric spectra

1. Introduction

Composites of carbon nanotubes (CNT) in polymeric matrices have attracted considerable attention in the research and industrial communities due to their good electrical conductivity, high stiffness, and high strength at relatively low CNT contents [1–8]. Such enhancements are attributed to the extraordinary electrical, mechanical, and thermal properties of CNT themselves. Carbon nanotubes can exist as single graphene sheet rolled up to cylinders, i.e. singlewalled carbon nanotubes (SWNT), or cylinders of multiple graphitic sheets, i.e. multiwalled carbon nanotubes (MWNT). In contrast to SWNT, where the conductivity depends on the chirality of the graphene sheets [9,10], MWNT materials are reported to be always electrically conductive and posses conductivities similar to copper [11]. In addition, MWNT have very high aspect ratios (length to diameter ratios), often in the range of 100–1000 [6,7]. Such high aspect ratios enable electrical percolation of the CNT within polymers to occur at very low CNT contents. Furthermore, CNT have exceptional mechanical properties, e.g. tensile strength as high as 20 GPa and moduli the order of 1 TPa [12–14]. Therefore, these kinds of fibers are excellent candidates for mechanical reinforcement. However, for this purpose nanotube/polymer interactions are necessary to improve the load transfer at the interface.

Effective utilization of nanotubes in composites with regard to enhancement of mechanical properties and electrical conductivity depends primarily on the ability to disperse the nanotubes homogeneously throughout the polymer matrix. However, homogeneous dispersion of nanotubes is difficult due to the intermolecular van der Waals interactions between the nanotubes, thus resulting in the formation of aggregates. This problem presents a major challenge irrespective of the method of composite preparation. In most of the cases, melt mixing is the preferred method of composite preparation, since aggregate formation can be minimized by appropriate application of shear during melt mixing [2,6,7].

On the other hand, characterization or quantification of

* Corresponding authors. Tel.: +49-6151-16-2404; fax: +49-6151-292855.
E-mail address: ialig@dki.tu-darmstadt.de (I. Alig).

0032-3861/03/$ - see front matter © 2003 Elsevier Science Ltd. All rights reserved.
doi:10.1016/S0032-3861(03)00451-8

the state of nanotube dispersion is also a difficult task. Optical microscopy only assesses very big agglomerates of nanotubes but is incapable of analysis at the submicron scale [2]. Methods based on the scanning and transmission electron microscopy (TEM) as well as atomic force microscopy are difficult to apply because of the extreme differences in nanotubes radial and axial dimensions and their complex shapes, e.g. curved and interconnected structures. This makes it difficult to observe an entire CNT or to distinguish between different CNTs [3,15–17]. Electrical measurements, however, can serve as a good indicator of the state of dispersion. For example, Ferguson et al. [7] compared the electrical conductivity of PC–MWNT composites obtained by mixing of a diluted masterbatch with different amounts of reprocessed compounds. Reprocessing in a Buss Kneader led to better dispersion of the nanotubes resulting in increased conductivity. This example demonstrates the sensitivity of the state of dispersion on processing condition; a topic not fully addressed to date in the literature.

The purpose of this work is to investigate the percolation structure, and, hence, the state of dispersion of MWNT in polycarbonate (PC) using dielectric spectroscopy. The morphology of MWNT composites is discussed and related to the electric and dielectric properties obtained for these materials. This relationship is of fundamental interest with respect to the conduction mechanism in CNT-filled systems. Dielectric spectroscopy represents a method which has been successfully applied to investigate the percolation structure of other conductive fillers, e.g. carbon black (CB), in polymeric matrices (see, e.g. [18–27] and references). Therefore, we expect that this method can lead to new insights in CNT filled systems, too. To our knowledge, use of dielectric spectroscopy with regard to CNT in earlier works was quite rare. There are reports on dielectric (optical) properties of carbon nanotubes at frequencies above 1 THz [28] and on carbon nanotube-loaded poly-(ethyl methacrylate) composites with 4–23 wt% SWNT in the frequency range between 500 MHz and 5.5 GHz [29]. These investigations were not focused on the issue of nanotube dispersion in a matrix or dispersion changes near the percolation composition and do not consider melt mixed polymeric composites.

2. Background

Two classes of models have been developed for the description of the frequency dependence of the complex conductivity $\sigma^*(\omega) = \sigma'(\omega) - i\sigma''(\omega)$ and the complex permittivity $\varepsilon^*(\omega) = \varepsilon'(\omega) - i\varepsilon''(\omega)$ (ω—angular frequency) in percolating systems: (i) the 'equivalent circuit model', which treats a percolation system as a random mixture of resistors and capacitors (alternatively: resistors–isolators, resistors–superconductors, conductor–insulator, etc.) [30–38] and (ii) models based on charge carrier diffusion on percolation clusters [36,39–49].

For two-component systems—percolation clusters of high conductivity (σ_1) embedded in a matrix of considerable lower conductivity (σ_2, $\sigma_2 \ll \sigma_1$)—macroscopic effective conductivity near the percolation threshold p_c can be written in the scaling form [30,34–37]:

$$\sigma(p,\omega) \propto \sigma_1 |p - p_c|^t \Phi_{\pm}\left(\frac{\sigma_2}{\sigma_1}|p - p_c|^{-(t+s)}\right), \quad (1)$$

where p is the concentration of conducting filler, Φ_+ and Φ_- denote scaling functions for $p > p_c$ and $p < p_c$, respectively, s and t are critical exponents. When treating a percolation system as a random mixture of resistors (R) and capacitors (C) having a characteristic relaxation time $\tau = 1/\omega_0 = RC$, scaling low Eq. (1) for the complex conductivity near the percolation threshold takes the form [35–37]:

$$\sigma^*(p,\omega) \propto \frac{1}{R}|p - p_c|^t \Phi_{\pm}\left(\frac{i\omega}{\omega_0}|p - p_c|^{-(t+s)}\right) \quad (2)$$

One of the main physical content of this key scaling law is the existence of a critical time scale

$$\tau_c(p) \propto \frac{1}{\omega_c(p)} \propto \frac{1}{\omega_0}|p - p_c|^{-(t+s)}, \quad (3)$$

that diverges as the percolation threshold is approached from both sides. In the static or DC (i.e. zero-frequency) limit the capacitors become insulators and the RC model becomes the conductor–insulator model [35]. Dependence of DC conductivity (σ_{DC}) on filler content (p) near the percolation threshold p_c can be described [30–32,36] by power laws:

$$\sigma_{DC}(p) \propto (p_c - p)^{-s} \quad (4)$$

for concentrations of filler below percolation threshold ($p < p_c$) and

$$\sigma_{DC}(p) \propto (p - p_c)^t \quad (5)$$

above the percolation threshold ($p > p_c$). For the frequency dependence of AC conductivity and the real part of the permittivity at the percolation threshold Bergman and Imry [37] derived the following laws:

$$\sigma'(\omega) \propto \omega^{\frac{t}{t+s}} \quad (6)$$

$$\varepsilon'(\omega) \propto \omega^{-\frac{s}{t+s}} \quad (7)$$

The composition dependence of the static permittivity $\varepsilon_s = \varepsilon'(\omega \to 0)$ was found [37,38]:

$$\varepsilon_s(p) \propto |p - p_c|^{-s} \quad (8)$$

for both $p > p_c$ and $p < p_c$. According to Eq. (8), the static permittivity is expected to diverge at the percolation threshold.

A wide variety of approaches have been applied to the determination of these exponents. Straley [50] calculated for

two-dimensional (2D) resistor lattice $s = t = 1.10 \pm 0.05$ and for three-dimensional (3D) resistor lattice $s = 0.70 \pm 0.05$, $t = 1.70 \pm 0.05$. Fish and Harris [51] applied the low-density series expansions for analysing of random resistor network and obtained $s = t = 1.43 \pm 0.02$ for 2D and $t = 1.95 \pm 0.03$ for 3D. Adler [52,53] reanalysed the data of Fish and Harris and calculated with series expansions method $t = 1.31 \pm 0.10$ for 2D and $t = 2.02 \pm 0.05$ for 3D. Alexander–Orbach conjecture [54] gives for 2D $t = 4/3 \cong 1.264$. Gingold and Lobb [55] employed finite-size scaling to analyse the critical behaviour of large three-dimensional random resistor lattices and reported for this case $t = 2.003 \pm 0.047$. Derrida et al. [56,57] and Herrmann et al. [58] used transfer-matrix calculations for analysing of random resistor network and obtained $s = t = 1.30 \pm 0.01$ for 2D and $s = 0.75 \pm 0.04$, $t = 1.9 \pm 0.1$ for 3D. Zabolitzky [59] used large-scale Monte-Carlo simulations and obtained results, which are very close to those from Derrida.

As mentioned above, an alternative to the 'equivalent circuit model' are models based on charge carrier motions on (fractal) percolation structures. This class of models does not directly include capacitances (e.g. to express gaps between clusters), but polarization effects are included by the finite time needed for the charge carriers to path through the percolation clusters. The frequency dependence of the conductivity is described by diffusion of conducting sites on percolation clusters. The correlation time τ_ξ, which a charge carrier needs to traverse a cluster of correlation length ξ, is given [35,40–44] by:

$$\tau_\xi \propto \xi^{d_w} \propto |p - p_c|^{-\nu d_w} \tag{9}$$

The exponent d_w is the effective fractal dimensionality of the random walk ('diffusion exponent') and ν is the exponent of the concentration dependence of the correlation length. The numerical value of the correlation length exponent for three-dimensional percolation was found [45,46,55] $\nu \cong 0.88$. Earlier for 2D-model it was found [60,61] $\nu = 4/3$. The value of τ_ξ increases with concentration for $p < p_c$ and decreases for $p > p_c$. For frequencies $\omega < \omega_\xi (\omega_\xi = 1/\tau_\xi)$ the length scale of the diffusive movements of charge carrier is considerably larger than the average cluster size and the charge carriers can explore different clusters within one period, i.e. the diffusion is normal and the conductivity becomes constant. For frequencies above ω_ξ the charge carriers visit only parts of the percolation cluster within one period and anomalous diffusion at the fractal percolation clusters takes place. The composition dependence of the static permittivity near the percolation threshold can be described [41–44] by:

$$\varepsilon_s \propto |p - p_c|^{-2\nu+\beta}, \tag{10}$$

for both, $p < p_c$ and $p > p_c$, where β is the percolation exponent, which characterises the probability that a site belongs to the infinite cluster (for $p > p_c$). It is important to note, that Eq. (10) has the same form as Eq. (8) with exponent $s' = 2\nu - \beta$. The numerical value for this critical exponent for 3D was found to be $s' = 1.33 \pm 0.01$ [53–56].

3. Experimental

3.1. Materials and composite preparation

A masterbatch of 15 wt% multiwalled carbon nanotube (MWNT) in PC was obtained in the form of granules from Hyperion Catalysis International, Inc. (Cambridge, MA, USA) [6,7]. The nanotubes were vapor grown and typically consist of eight to fifteen graphitic layers wrapped around a hollow 5 nm core [6]. They are produced as agglomerates and exist as curved intertwined entanglements [8]. Typical diameters range from 10–15 nm while lengths are between 1 and 10 μm. The density is approximately 1.75 g/cm^3 [1]. The masterbatch was diluted with the same PC, as used in the masterbatch (zero shear viscosity of 600 Pa s at 260 °C) using melt mixing in a DACA Micro Compounder (DACA Instruments, Goleta, CA, USA) at 260°C [16,17]. This compounder has a capacity of 4.5 cm^3 and consists of two conical co-rotating screws with a bypass allowing the material to circulate for defined periods. Prior to mixing, the materials were dried for a minimum of 16 h at 80 °C in a vacuum oven. The masterbatch was diluted by the PC to obtain concentrations of 0.5, 1, 1.5, 2, 3, 4 and 5 wt% MWNT in PC, which corresponds to 0.34, 0.68, 1.03, 1.38, 2.08, 2.78 and 3.48 vol%. In the first set of experiments, mixing was performed at a rotational speed of 150 rpm applied for 5 min and MWNT content was varied. After the mixing, the extruded material was taken out using the set screw speed through the heated cylindrical die into air without additional cooling or drawing. In the second set of experiments, MWNT content was fixed at 1.0 and 1.5 wt% while the processing conditions were varied. The mixing time was prolongated to 15 min; in addition a lower screw speed of 50 rpm was used with 15 min mixing. Sheets with a thickness of 350 μm were formed by compression moulding from extruded strands at 260 °C using a Vogt-press. The strands were heated to 260 °C for about 2 min, pressed with a force of about 50 kN for 1 min and cooled to room temperature. The samples used in the dielectric measurements were discs with diameter of 20 mm cut from these sheets. Gold layers were sputtered onto both flat sides of the samples as electrodes.

3.2. Dielectric measurements

The dielectric measurements were performed in a frequency range from 10^{-4} to 10^7 Hz using a frequency response analysis system consisting of a computer-controlled Solartron SI 1260 Impedance/Gain-Phase Analyzer and a Novocontrol broadband dielectric converter at room temperature. For the samples with 1.5 and 2.0 wt% (mixed

at 150 rpm for 5 min) the capacity was additionally measured by HP 4284 LCR-Meter.

In this paper, the spectra of the real part of the complex conductivity (σ'), the real (ε') and imaginary part (ε'') of the complex dielectric permittivity are presented. $\sigma''(\omega)$ is not discussed, since we restrict our discussion to ε', which is more common.

4. Results and discussion

4.1. Permittivity and conductivity spectra for different MWNT content

Fig. 1 shows the complex permittivity and the conductivity spectra for different MWNT loadings in PC. All samples of this set have been prepared with a screw speed of 150 rpm for 5 min. For samples with more than 1 wt% MWNT, the lowest experimental frequency was chosen to be 0.1–1 Hz, since the DC conductivity plateau was clearly achieved.

Due to the high AC conductivity of the samples with contents higher than 2 wt% MWNT, it was not possible to measure reasonable values of ε' for these compositions. However, it is clearly seen in Fig. 1, that the curves can be distinguished between the two groups. The composites with 0.5 and 1.0 wt% MWNT have a nearly constant ε' value and

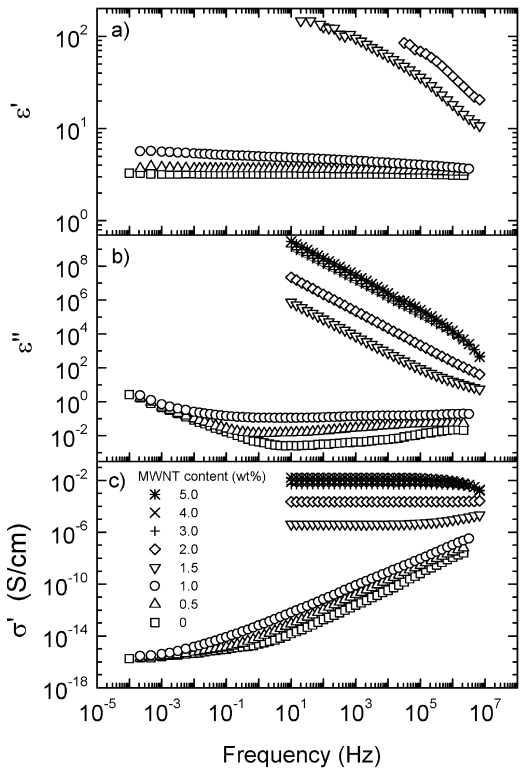

Fig. 1. The effect of frequency on the (a) real part ε', (b) imaginary part ε'' of the complex permittivity, and (c) AC conductivity σ' for PC composites of varying MWNT content. All samples of this set have been mixed for 5 min with a screw speed of 150 rpm.

only small changes in ε'', whereas, composites with MWNT loading higher than 1.0 wt% show a significantly different behaviour. Here, ε' and ε'' decrease with increasing the frequency. The power law behaviour of $\varepsilon''(\omega)$ for frequencies lower than some critical frequency is directly related to the DC conductivity ($\sigma_{DC} = \omega\varepsilon''(F < f_c)$). A significant difference between the two groups is also visible in DC conductivity ($\sigma_{DC} = \sigma'(\omega \rightarrow 0)$ (see Fig. 1(c)), which is a measure of the long range movements of the charge carriers.

Fig. 2 shows the extrapolated static values of the DC conductivity versus the MWNT content. For accurate definition of σ_{DC} for the samples with 0, 0.5 and 1.0 wt% MWNT, the values of σ' at frequencies lower then 10^{-4} Hz should be measured (see Fig. 1). Such measurements would increase the measuring time significantly and are addressed to future investigations. As an estimation for σ_{DC} we used for these samples the values of σ' at lowest measured frequency.

The percolation composition (p_c) clearly occurs between 1.0 and 1.5 wt%. At this composition, the conductivity changes significantly (over more than 10 decades). In other words, below this concentration the composites are very resistant to electrical flow, whereas above this value the composites are conductive. In order to get an estimate for p_c and the critical exponent t, we fitted the σ_{DC} data for $p > p_c$ to Eq. (5). This was done by variation of p_c in the interval from 1.10 to 1.49 in steps of 0.01. For each value of p_c the value of t has been determined from the slope of the linear relation of σ_{DC} and $p-p_c$ on a log–log scale. The lowest value of the root mean square error was found for $p_c = 1.44 \pm 0.05$ with the exponent $t = 2.1 \pm 0.1$ (see insert in Fig. 2). The curve for $p < p_c$ in Fig. 2 was calculated from Eq. (4) with $p_c = 1.44$ (obtained above) and $s = 0.73$ (see Refs. [35,36,44,58]). For an exact estimation of the exponent s for $p < p_c$ a larger number of samples should be investigated and σ' at frequencies lower than 10^{-4} Hz should be measured. The value $t = 2.1 \pm 0.1$ calculated here for the MWNT composites is in agreement with the

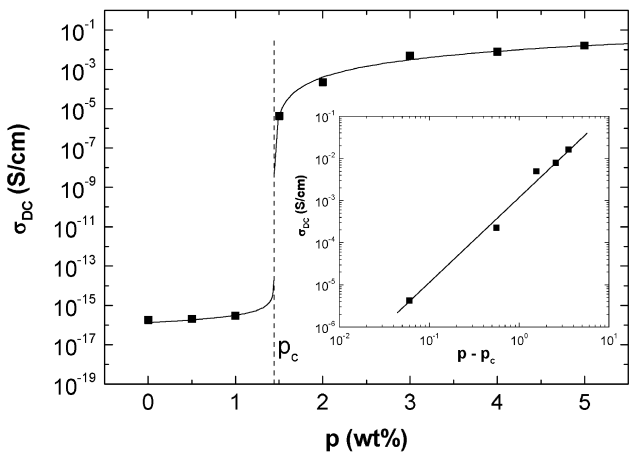

Fig. 2. DC conductivity σ_{DC} versus MWNT concentration p (wt%) in PC for the set of samples shown in Fig. 1. The insert shows the values of σ_{DC} above the percolation concentration p_c versus $(p-p_c)$.

theoretical value of $t \cong 2.0$ for a percolation network in three dimensions [43,44,51–55], whereas for CB polymer composites the experimental values for t are typically higher [26,27,62]. The latter was explained by the internal structure of CB aggregates [62] and by cluster–cluster aggregation [63–65]. Recently, we showed that the dielectric properties of natural rubber containing CB for $p > p_c$ can be explained by the assumption of a secondary aggregation structure [26,27]. The agreement of the value of exponent t for our CNT composites with the percolation theory thus may suggest the absence of similar (fractal) superstructures and more likely is related to the large aspect ratio of CNT as well its low absolute concentration near p_c. This, however, does not exclude the existence of aggregates or bundles of CNT. According to the high aspect ratio of the MWNT used, a concentration between 1 and 2 wt% for the percolation threshold is still high. Therefore, only part of the CNT is involved in the formation of the conducting network.

A second DC quantity that can be derived from the experimental data is the static permittivity $\varepsilon_s = \varepsilon'(\omega \rightarrow 0)$. Static permittivity is expected to increase with increasing filler content when approaching p_c for small concentrations and to decrease above the percolation threshold (see Eqs. (8) and (10)). The extrapolated values of $\varepsilon'(\omega \rightarrow 0)$ versus the MWNT content are shown in Fig. 3.

Although, the static permittivity data are incomplete due to large measurement error for the samples with 1.5 and 2.0 wt% and missing values above the experimental limit for higher MWNT contents, it is obvious that ε_s remains constant or perhaps increases above p_c but does not decrease as expected from Eqs. (8) and (10). Such behaviour has been reported earlier for polymer composites containing CB [18,26,27,66,67] and was attributed to 'micro capacitors' remaining in the sample above p_c. For PC–MWNT composites the value of ε_s ($p > p_c$) is in the order of 10^2, whereas the typical values for CB-rubber composites are in the order of 10^3–10^4 [26,27]. The lower value of ε_s for MWNT is an indication of a considerably smaller number of conducting particles per volume compared to CB composites. Together with the high aspect ratio this may result in a smaller number of 'micro capacitors' per volume. These 'micro capacitors' are assumed to be formed by gaps between CNT (similar to the 'bound rubber' in CB networks). Another possibility for formation of capacitances is parallel strength and free ends of the percolation structure. The solid lines in Fig. 3 are calculated from Eq. (8) with $p_c = 1.44$ (estimated above) and the theoretical value of $s = 0.73$ for percolation network formed by a random mixture of complex resistors (see Refs. [35,36,44,58]). On the other side, the charge carrier diffusion on percolation structures is expressed by Eq. (10) with the exponent $2\nu - \beta \cong 1.33$ [43–46]. The dotted lines in Fig. 3 correspond to this model. For the limited number of data points, it is impossible to differentiate between different models (however, fitting with the exponent 0.73 seems to be closer to our experimental data).

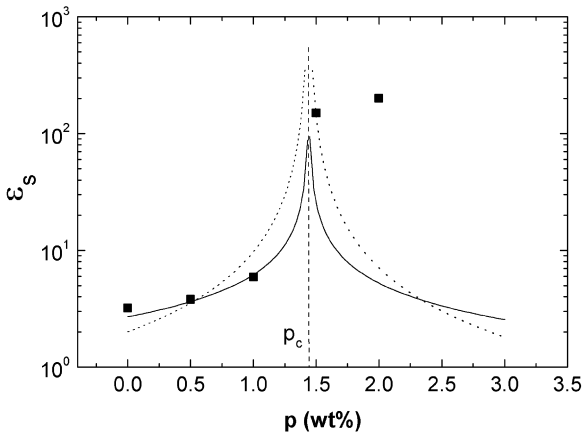

Fig. 3. Static permittivity $\varepsilon_s = \varepsilon'(\omega \rightarrow 0)$ versus MWNT concentration p (wt%) in PC for the samples shown in Fig. 1.

Another quantity which can be extracted from the frequency dependence of conductivity, is the crossover frequency $f_c = \omega_c/2\pi$, defined as the frequency at which AC conductivity differs from the DC plateau. For charge carrier diffusion on percolation structures, f_c is related to the transition from normal diffusion ($\sigma'(f < f_c) = \sigma_{DC} =$ const) to anomalous diffusion ($\sigma'(f > f_c) \propto \omega^n$). This crossover can be observed only for some samples in the frequency range of the experiments (see Table 1).

For a quantitative analysis and a test of the theoretical predictions, a larger number of samples having well defined mixing conditions (see next chapter) and compositions close to the percolation threshold (here: between 1 and 1.5 wt% MWNT) are required. Investigations of this sort are in progress.

4.2. The effect of melt mixing conditions on the permittivity and conductivity spectra near the percolation threshold

Fig. 4 shows the complex permittivity and conductivity spectra for the composites with 1.0 wt% (open symbols) and 1.5 wt% MWNT (closed symbols) processed at 150 rpm for 5 and 15 min and at 50 rpm for 15 min.

4.2.1. Composites with 1.0 wt% MWNT

For the composites with 1.0 wt%, increasing mixing time from 5 to 15 min at 150 rpm leads to a significant change in DC conductivity from 2.5×10^{-16} to 5.3×10^{-8} S/cm (see Table 1). The comparison of these values (Fig. 4) with those of Fig. 2 leads to the conclusion that the sample corresponding to a mixing time of 5 min is below the percolation threshold p_c, whereas the sample mixed for 15 min is above p_c. Since both samples have the same composition, this result clearly indicates that p_c depends on mixing time. A second possibility to change mixing energy is to vary screw speed, which is related to shear rate. Reduction of the screw speed for the composite with 1.0 wt% MWNT from 150 to 50 rpm (mixing time 15 min) shows slightly lower DC conductivity (see Fig. 4 and Table

Table 1
The influence of mixing conditions on characteristic values of permittivity and conductivity spectra

Sample	MWNT content (wt%)	Screw speed (rpm)	Mixing time (min)	Crossover frequency, f_c (Hz)	DC conductivity, σ_{DC} (S/cm)
Set II/1	1.0	150	5	5.2×10^{-3}	2.5×10^{-16}
Set II/2	1.0	150	15	6.1×10^{4}	5.3×10^{-8}
Set II/3	1.0	50	15	1.1×10^{3}	8.7×10^{-10}
Set II/4	1.5	150	5	2.2×10^{5}	4.1×10^{-6}
Set II/5	1.5	150	15	6.4×10^{4}	9.1×10^{-7}
Set II/6	1.5	50	15	$> 10^{6}$	2.2×10^{-4}

1). On the other hand, σ_{DC} is still much higher than for the composite mixed at 150 rpm for 5 min. From the values of the DC conductivity and the complex permittivity curves, it can be concluded that the sample mixed at 50 rpm for 15 min also is above the percolation threshold p_c.

According to Eqs. (3) and (9), the value of the crossover frequency f_c is a measure of the absolute distance $|p-p_c|$ of the actual composition p from p_c ($f_c \rightarrow 0$ for $p \rightarrow p_c$). For the composites with 1.0 wt% MWNT, the higher value of the sample mixed at 150 rpm for 15 min indicates a larger distance from p_c than of the sample mixed for 5 min, whereas the first sample is below p_c and the second above p_c. The decrease of f_c with reduction of screw speed from 150 to 50 rpm (mixing time 15 min) results from a higher value of p_c due to worse dispersion of MWNT at the lower mixing speed.

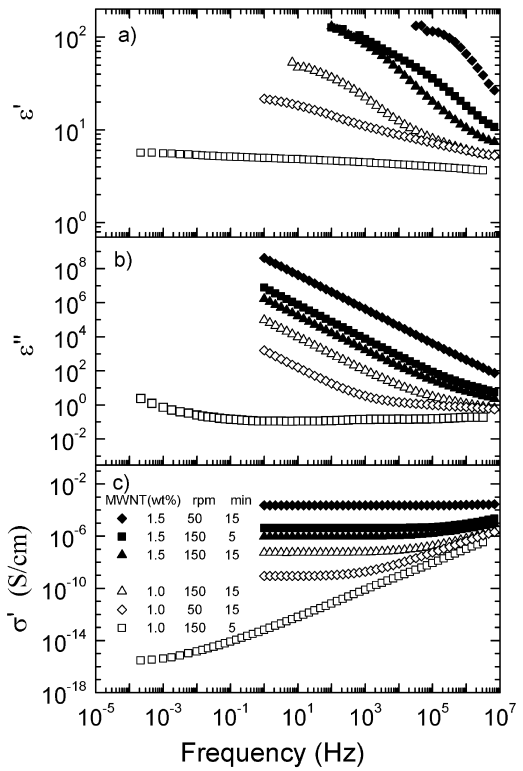

Fig. 4. The effect of mixing time and screw speed on the (a) real part ε', (b) imaginary part ε'' of the complex permittivity, and (c) AC conductivity σ' versus frequency for the composites with 1.5 wt% (closed symbols) and 1.0 wt% MWNT (open symbols).

The ε' and ε'' curves in Fig. 4 show the expected decrease with increasing frequency below f_c. For a fixed frequency ($f < f_c$) the values of ε' and ε'' increase with mixing time (screw speed 150 rpm). This can be explained by the shift of the crossover frequency f_c of about seven decades, which is again related to the distance $|p-p_c|$. The increase of $\varepsilon'(f < f_c)$ with mixing time is additionally caused by a change in the static permittivity ε_s as discussed above. The reduction of the screw speed from 150 to 50 rpm (mixing time 15 min) result in a slight decrease of the ε' and ε'' values for a given frequency related to the increase in p_c.

The results for the samples with 1.0 wt% MWNT indicate that, at least for low MWNT loadings, mixing time is the more important factor to enhance dispersion as compared to the screw speed. Appropriate mixing conditions can induce a transformation of a non percolated system into a percolated structure. One possible explanation is that longer mixing time promote polymer diffusion in-between MWNT aggregates of the masterbatch. According to the literature, increasing mixing time is expected to enhance dispersion. Ferguson et al. [7] showed that reprocessing of PC–MWNT formulations in a Buss Kneader resulted in increased conductivity which can be attributed to better dispersion of the nanotubes. Andrews et al. [2] showed that an increase of mixing energy, achieved by increased mixing time (up to 25 min) at a given screw speed, enhances dispersion (as characterized by light microscopy) but reduces the MWNT length up to 25%. In their experiments 0.5 vol% MWNT was mixed into polystyrene using a Haake Polylab Rheomix. The MWNT lengths were assessed by dissolving the composites in acetone and observing the tubes using TEM. Our dielectric results, which can be correlated to the state of dispersion, agree with Andrews finding and lead to the conclusion that, for the sample with 1.0 wt% MWNT, the better dispersion by an increase of mixing time and use of higher screw speed prevails over the reduction of MWNT length. The latter is expected to shift the percolation threshold to higher compositions, since the aspect ratio of MWNT is decreased.

4.2.2. Composites with 1.5 wt% MWNT

Fig. 4 shows that the samples with 1.5 wt% MWNT are clearly above the percolation threshold. Regardless of the mixing conditions each sample is conductive. The influence

of mixing conditions for these samples is different from that for 1.0 wt% MWNT composites. The experimental results (see Fig. 4 and Table 1) show that an increase of the mixing time from 5 to 15 min at high shear rate (screw speed 150 rpm) slightly reduces both, the DC conductivity σ_{DC} and the crossover frequency f_c, whereas a reduced screw speed at higher mixing time (50 rpm, 15 min) enhances the DC conductivity significantly and shifts f_c to higher values (above the range of our experiments). This is consistently expressed in the shifts of $\varepsilon'(f)$ and $\varepsilon''(f)$ curves, which can be discussed in agreement with the arguments given above for the samples containing 1.0 wt% MWNT. A detailed analysis of the complex permittivity curves, e.g. in the frame of 'equivalent circuit models' should be addressed to a separate study.

The values of σ_{DC} and f_c are again a measure of the distance $|p-p_c|$ of the actual composition p from p_c. From the experimental findings, we can conclude that p_c is increasing with mixing time and screw speed. As shown in our previous papers [17,68], the melt viscosity exhibits a step increase with MWNT content at the percolation threshold. In other words, the high mechanical energy required in mixing composites above p_c is a consequence of MWNT percolation. Above p_c, nanotube breakage, as discussed in Ref. [2], becomes an important factor. For a given composition the increase of nanotube breakage causes an increase of p_c because the aspect ratio of CNT is reduced. The increase of p_c with mixing time and screw speed due to nanotube breakage is expected to prevail over the decrease of p_c due to better dispersion of MWNT. The results measured for σ_{DC} in this study are consistent with the measurements of volume resistivity on 60 mm sheets using a Keithley electrometer Model 6517 [69], which can be considered as an additional proof of the discussed tendencies.

5. Summary and conclusions

In this paper, we have presented frequency dependent dielectric relaxation experiments on multiwalled carbon nanotube (MWNT)/PC composites. Both, the influence of the carbon nanotube content and the melt processing conditions on the complex permittivity spectra and the frequency dependent conductivity were studied. The main results can be summarized as follows:

(1) The percolation threshold of MWNT in melt mixed PC composites prepared in a Micro Compounder at 260 °C, 150 rpm, 5 min occurred at ~1.4 wt%, corresponding to a change in the DC conductivity of more than ten decades. The percolation critical exponent t obtained from fitting the composition dependence of the DC conductivity above the percolation threshold is consistent with the suggestions of percolation theory for a three dimensional percolation structure. The static permittivity was found to increase with MWNT content below the percolation threshold, as expected, whereas its value does not decrease above p_c. This is similar to the behaviour of CB polymer composites and is addressed to remaining (micro-) capacitors formed at the contacts between CNT aggregates or bundles.

(2) Increase of the mixing time can improve the distribution of MWNT in the polymer matrix considerably. At concentrations near the percolation threshold, enhanced mixing time can transform the system from a non percolated into a percolated one. The effect of mixing time is explained by the time necessary for diffusion of the polymer chains between the MWNT aggregates or bundles of the masterbatch. Both DC conductivity and the crossover frequency have been found to be sensitive to the changes of the critical nanotube content at percolation threshold $p_c(t_{mix})$ with mixing time t_{mix}.

(3) The screw speed had a significant effect on the dispersion of MWNT. However, it was found to act differently for compositions below and above the percolation threshold p_c. At MWNT contents below p_c, increased screw speed induces better dispersion, whereas above p_c the efficient transfer of mechanical energy due to nanotube network formation can lead to enhanced breakage of the MWNT and decrease of DC conductivity and crossover frequency.

The results presented here clearly show that dielectric spectroscopy is a viable method for the characterization of the state dispersion of MWNT in melt processed nanocomposites. To test power law models for predicting electrical percolation behaviour it is necessary to prepare a more complete series of samples with smaller differences in CNT content, especially for compositions close to the percolation threshold. Furthermore, systematic investigations of the dependence of conductivity on temperature are expected to provide a deeper insight in the conduction mechanisms of CNT polymer composites, e.g. how does temperature effect the level of hopping or tunneling and the composites' semiconductivity. From a polymer processing standpoint experiments involving a more systematic variation of mixing conditions and different polymers and/or additives, e.g. those which provide better dispersion of CNT, are of interest.

Acknowledgements

The authors would like to thank Hyperion Catalysis International, Inc. for providing the masterbatch and the polycarbonate and the Forschungsgesellschaft Kunststoffe, the Fond der Chemischen Industrie, and the European Science (ESF) foundation for financial support.

References

[1] Shaffer MSP, Windle AH. Adv Mater 1999;11(11):937–41.
[2] Andrews R, Jacques D, Minot M, Rantell T. Macromol Mater Engng 2002;287:395–403.
[3] Cooper CA, Ravich D, Lips D, Mayer J, Wagner HD. Compos Sci Technol 2002;62:1105–12.
[4] Haggenmueller R, Gommans HH, Rinzler AG, Fischer JE, Winey KI. Chem Phys Lett 2000;330:219–25.
[5] Jin Z, Pramoda KP, Xu G, Goh SH. Chem Phys Lett 2001;337:43–7.
[6] Hagerstrom JR, Greene SL. Electrostatic dissipating composites containing hyperion fibril nanotubes. Commercialization of nanostructured materials, Miami, USA, April.; 2000.
[7] Ferguson DW, Bryant EWS, Fowler HC. ESD Thermoplastic product offers advantages for demanding electronic applications, ANTEC'98. 1998;1219–22.
[8] Sandler J, Shaffer MSP, Prasse T, Bauhofer W, Schulte K, Windle AH. Polymer 1999;40:5967–71.
[9] Wildöer JWG, Venema LC, Rinzler AG, Smalley RE, Dekker C. Nature 1998;391:59–62.
[10] Odom TW, Huang JL, Kim P, Lieber C. Nature 1998;391:62–4.
[11] Kaiser AB, Düsberg G, Roth S. Phys Rev B 1998;57(3):1418–21.
[12] Qian D, Dickey EC, Andrews R, Rantell T. Appl Phys Lett 2000; 76(20):2868–70.
[13] Schadler LS, Giannaris SC, Ajayan PM. Appl Phys Lett 1998;73(26): 3842–4.
[14] Salvetat J-P, Briggs GAD, Bonard J-M, Bacsa RR, Kulik AJ, Stöckli T, Burnham NA, Forró L. Phys Rev Lett 1999;82(5):944–7.
[15] Sennett M, Welsh E, Wright JB, Li WZ, Wen JG, Ren ZF. Appl Phys A 2003;76:111–3.
[16] Pötschke P, Bhattacharyya AR, Goering H. Melt mixing of polycarbonate/multi wall carbon nanotubes composites. Compos Interfaces 2003; in press.
[17] Pötschke P, Bhattacharyya AR, Janke A. Melt mixing of polycarbonate with multiwalled carbon nanotubes: microscopic studies on the state of dispersion. Submitted for publication.
[18] McLachlan DS, Heaney MB. Phys Rev B 1999;60(18):12746–51.
[19] Chakrabarty RK, Bardhan KK, Basu A. J Phys Condensed Matter 1993;5:2377–88.
[20] Adriaanse LJ, Reedijk JA, Teunissen PAA, Brom HB, Michels MAJ, Brokken-Zijp JCM. Phys Rev Lett 1997;78(9):1755–8.
[21] Connor MT, Roy S, Ezquerra TA, Balta Calleja F. J Phys Rev B 1998; 57(4):2286–94.
[22] Kawamoto H. Carbon black-polymer composites. In: Sichel EK, editor. The physics of electrically conductive conducting composites. New York: Decker; 1982. p. 135–62.
[23] Schwartz G, Cerveny S, Marzocca AJ. Polymer 2000;41:6589–95.
[24] Ouyang GB. Kautschuk Gummi Kunststoffe 2002;55(3):104–13.
[25] Jäger K-M, McQueen DH, Tchmutin IA, Ryvkina NG, Klüppel M. J Phys D: Appl Phys 2001;34:2699–707.
[26] Kastner A. Dielektrische Charakterisierung rußgefüllter Elastomere, PhD Thesis, Darmstadt, 2002.
[27] Alig I, Kastner A, Heinrich G, Klüppel M. e-Polymers 2002;033.
[28] Lin MF, Shung KWK. Phys Rev B 1994;50(23):17744–7.
[29] Grimes CA, Mungle C, Kouzoudis D, Fang S, Eklund PC. Chem Phys Lett 2000;319:460–4.
[30] Efros AL, Shklovskii BI. Phys Status Solidi b 1976;76:475–85.
[31] Kirkpatrick S. Rev Mod Phys 1973;45:574–88.
[32] Kirkpatrick S. Phys Rev Lett 1976;36(2):69–72.
[33] Stephen MJ. Phys Rev B 1978;17(11):4444–53.
[34] Straley JP. J Phys C: Solid State Phys 1976;9:783–95.
[35] Clerc JP, Giraud G, Laugier JM, Luck JM. Adv Phys 1990;39(3): 191–309.
[36] Stauffer D, Aharony A. Introduction to percolation theory. London: Taylor and Francis; 1994.
[37] Bergman DJ, Imry Y. Phys Rev Lett 1977;39(19):1222–5.
[38] Stroud D, Bergman DJ. Phys Rev B 1982;25(3):2061–4.
[39] Stauffer D. Phys Rep 1979;54(1):1–74.
[40] Straley JP. J Phys C: Solid State Phys 1980;13:2991–3002.
[41] Gefen Y, Aharony A, Mandelbrot BB, Kirkpatrick S. Phys Rev Lett 1981;47(25):1771–4.
[42] Gefen Y, Aharony A, Alexander S. Phys Rev Lett 1983;50(1):77–80.
[43] Bunde A, Havlin S. In: Bunde A, Havlin S, editors. Fractals and disordered systems. Berlin: Springer; 1996.
[44] Sahimi M. Applications of percolation theory. London: Taylor and Francis; 1994.
[45] Heermann DW, Stauffer D. Z Phys B 1981;44:339.
[46] Ziff RM, Stell G. LaSC, University of Michigan, Report No. 88 4, 1988, Footnote 26.
[47] Scher H, Lax M. Phys Rev B 1973;7(10):4491–519.
[48] Maass P, Meyer M, Bunde A. Phys Rev B 1995;51(13):8164–77.
[49] Hong DC, Halvin S, Herrmann HJ, Stanley HE. Phys Rev B 1984; 30(7):4083–6.
[50] Straley JP. Phys Rev B 1977;15(12):5733–7.
[51] Fish R, Harris AB. Phys Rev B 1978;18(1):416–20.
[52] Adler J, Meir Y, Aharony A, Harris AB, Klein L. J Stat Phys 1990;58: 511.
[53] Adler J. J Phys A: Math Gen 1985;18:307–14.
[54] Alexander S, Orbach R. J Phys Lett (Paris) 1982;43:L625.
[55] Gingold DB, Lobb CJ. Phys Rev B 1990;42(13):8220–4.
[56] Derrida B, Vannimenus J. J Phys A: Math Gen 1982;15:L557–64.
[57] Derrida B, Stauffer D, Herrmann HJ, Vannimenus J. J Phys Lett (Paris) 1983;44:L701.
[58] Herrmann HJ, Derrida B, Vannimenus J. Phys. Rev B 1984;30(7): 4080–2.
[59] Zabolitzky JG. Phys. Rev. B 1984;30(7):4077–9.
[60] Den Nijs MPM. J Phys A: Math Gen 1979;12(10):1857–68.
[61] Nienhuis B. J Phys A: Math Gen 1982;15:199–213.
[62] Karásek L, Meissner B, Asai S, Sumita M. Polym J 1996;28(2): 121–6.
[63] Kolb M, Botet R, Jullien R. Phys Rev Lett 1983;51(13):1123–6.
[64] Klüppel M, Heinrich G. Rubber Chem Technol 1995;68:623–51.
[65] Klüppel M, Schuster RH, Heinrich G. Rubber Chem Technol 1997; 70:243–55.
[66] Flandin L, Prasse T, Schueler R, Schulte K, Bauhofer W, Cavaille J-Y. Phys Rev B 1999;59(22):14349–55.
[67] Tchmutin IA, Ponomarenko AT, Shevchenko VG, Ryvkina NG, Klason C, McQueen DH. J Polym Sci B: Polym Phys 1998;36: 1847–56.
[68] Pötschke P, Fornes TD, Paul DR. Polymer 2002;43:3247–55.
[69] Pötschke P, Bhattacharyya AR. Polym Preprints 2003;44(1):760–1.